Soft Matter

PAPER

View Article Online
View Journal | View Issue

Check for updates

Cite this: *Soft Matter*, 2018, **14**, 1162

Complex patchy colloids shaped from deformable seed particles through capillary interactions†

V. Meester and D. J. Kraft *

We investigate the mechanisms underlying the reconfiguration of random aggregates of spheres through capillary interactions, the so-called "colloidal recycling" method, to fabricate a wide variety of patchy particles. We explore the influence of capillary forces on clusters of deformable seed particles by systematically varying the crosslink density of the spherical seeds. Spheres with a poorly crosslinked polymer network strongly deform due to capillary forces and merge into large spheres. With increasing crosslink density and therefore rigidity, the shape of the spheres is increasingly preserved during reconfiguration, yielding patchy particles of well-defined shape for up to five spheres. In particular, we find that the aspect ratio between the length and width of dumbbells, L/W, increases with the crosslink density (cd) as $L/W = B - A\cdot\exp(-\mathrm{cd}/C)$. For clusters consisting of more than five spheres, the particle deformability furthermore determines the patch arrangement of the resulting particles. The reconfiguration pathway of clusters of six densely or poorly crosslinked seeds leads to octahedral and polytetrahedral shaped patchy particles, respectively. For seven particles several geometries were obtained with a preference for pentagonal dipyramids by the rigid spheres, while the soft spheres do rarely arrive in these structures. Even larger clusters of over 15 particles form non-uniform often aspherical shapes. We discuss that the reconfiguration pathway is largely influenced by confinement and geometric constraints. The key factor which dominates during reconfiguration depends on the deformability of the spherical seed particles.

Received 11th October 2017,
Accepted 21st December 2017

DOI: 10.1039/c7sm02020a

rsc.li/soft-matter-journal

Open Access Article. Published on 04 January 2018. Downloaded on 1/15/2026 5:10:06 AM.
This article is licensed under a Creative Commons Attribution 3.0 Unported Licence.

Introduction

Patchy colloids are excellent building blocks for self-assembly, since their anisotropy in surface chemistry allows them to form complex structures.[1–3] While spheres with isotropic interactions only crystallize in a randomly stacked hexagonal closed packed structure, particles with a single patch already assemble into micelles[4] and tubules.[5,6] Particles with multiple patches have been predicted to exhibit an even richer phase behavior,[7,8] such as crystallization into dense diamond,[9] body-centered-cubic and face-centered-cubic[10] lattices as well as open networks.[11] A directional interaction profile also has exciting potential for mimicking polymer chain formation,[12] complex protein assemblies[13,14] and the bottom up construction of smart materials.[15,16] Patchy colloids with multiple interaction sites have been experimentally realized by, for example, partial coverage of the surface with a droplet[17,18] or a second type of colloid.[19,20] Self-assembly of such particles has been achieved by site-specific interactions based on DNA-linkers,[21,22] metal coordination,[23] hydrophobic interactions,[24] capillary bridges,[25] and depletion forces.[4]

We have recently contributed to the available synthetic approaches with a strategy based on reconfiguring random aggregates of spheres into patchy particles.[26] The technique relies on the introduction of apolar droplets to the contact areas of the aggregated spheres dispersed in aqueous solution. These droplets enable rotational mobility and induce a reorganization of the spheres driven by capillary forces. By merging these capillary bridges the interfacial energy is minimized. The cluster-spanning droplet connects and partially shields the seed spheres, which creates patches. After polymerization of the droplet, this leads to patchy particles with a compact shape. The advantages of our "colloidal recycling" approach are that it can be performed in bulk in aqueous, non-toxic media and that various types of patchy particles can be obtained by variation of the initial seed particles and/or organic solvent.

In our previous study we observed that the location of the patches and the overall particle geometry is unique for each number of seed particles for up to $N = 5$ spheres. Above $N = 5$, we found that the sphere arrangement and thus the patch location depended on the type of seed particles we used. For example, we observed both a polytetrahedral and an octahedral arrangement for six spheres. In previous experiments, theoretical models and numerical calculations it was found that the preference for a certain geometry can be determined by various factors

Soft Matter Physics, Huygens-Kamerlingh Onnes Laboratory, Leiden University, PO Box 9504, 2300 RA Leiden, The Netherlands. E-mail: kraft@physics.leidenuniv.nl

† Electronic supplementary information (ESI) available. See DOI: 10.1039/c7sm02020a

This journal is © The Royal Society of Chemistry 2018

Open Access Article. Published on 04 January 2018. Downloaded on 1/15/2026 5:10:06 AM.
This article is licensed under a Creative Commons Attribution 3.0 Unported Licence.

such as maximizing the number of contacts,[27] the interaction profile,[28,29] entropy,[30] capillary forces,[31] packing constraints,[32] and interfacial phenomena.[33]

The observation of both a polytetrahedral and octahedral arrangement in our experiments implies that the physical or chemical properties of the seed particles influence the reconfiguration process by affecting either the kinetic pathway and/or the free energy landscape of the final configuration. In our previous work we suspected that the particle rigidity was the crucial difference between the seed particles, but since they had been prepared following different methods other factors could not systematically be excluded. Clearly, the key to tailor our method to create patchy particles with complex and new patch arrangements is a better understanding of the assembly pathway.

We here investigate the reconfiguration process and use this knowledge to assemble a wide variety of complex patchy particles. We analyse how spheres of different rigidity are deformed during reconfiguration and how this affects the geometry and final shape of the cluster. Quantitative results are presented of the deformation of spheres with different crosslink densities. We also study the influence of the capillary forces on the reconfiguration pathway of clusters constructed from six or more spheres. The soft and rigid spheres reconfigure to different shapes, which points to different assembly pathways.

Results and discussion

The colloidal recycling method

We studied the shape and assembly pathway of patchy particles constructed from spheres of varying rigidity. These patchy colloids were obtained by applying the colloidal recycling method,[26] illustrated in Fig. 1A, to spheres with different crosslink densities. Here, colloidal aggregates with a controlled size distribution are formed by diffusion limited aggregation induced by the addition of salt to electrostatically stabilized colloidal spheres. Reconfiguration of the randomly shaped aggregates is induced by the addition of organic solvent, which is deposited in small droplets at the contact area between the spheres. This results in the formation of capillary bridges. The droplets decrease the attractive van der Waals forces between the particles and lubricate the contact area, which enables rotational mobility of the spheres in the aggregate. Since capillary forces dominate, the small droplets coalesce into one cluster-spanning droplet to decrease the interfacial energy.[34] The aggregates therefore reconfigure into compact shapes yielding patchy particles with well-defined geometries. Since this process is purely based on reconfiguration of the initial aggregates, the size distribution of the patchy particles is equivalent to that of the aggregates.[26] The size distribution can therefore be tuned by experimental parameters during the aggregation step such as the colloid concentration, the salt concentration, the surface charge of the colloids and the aggregation time, t_a. The universality of this method with respect to the particle properties of the seeds, allows using various types of seed particles.

Spherical, anisotropic and patchy particles of deformable spheres

During the reconfiguration process strong capillary forces act on the spheres in the cluster. With increasing crosslink density of the polymer colloids, the rigidity of the polymer network increases and thus the ability of the particle to resist swelling and deformation induced by the capillary forces.[35,36] We therefore expect that the deformability of the seed particles influences the size of the contact area between spheres and the final shape of the reconfigured cluster (Fig. 1B and C). To investigate how spheres of varying rigidity are influenced by capillary forces we studied particles made from spherical seed particles with a crosslink density (cd) of 0.2, 0.5, 0.7, 1.4, 2.1, 3.0, 4.3 or 8.3% v/v (volume of crosslinking agent/volume of polystyrene) and a diameter of approximately 1.5 μm, see Table 1 and Fig. S1 (ESI†) for details and methods. The concentration of the organic solvent and other experimental parameters were equal in all experiments.

We found that the shapes of the reconfigured particles strongly depend on the crosslink density of the seeds. Aggregates of spheres with a low crosslink density, cd = 0.2% v/v, and thus low rigidity, were deformed so strongly by surface tension that the shape of the individual spheres could not be maintained. Instead, the seed

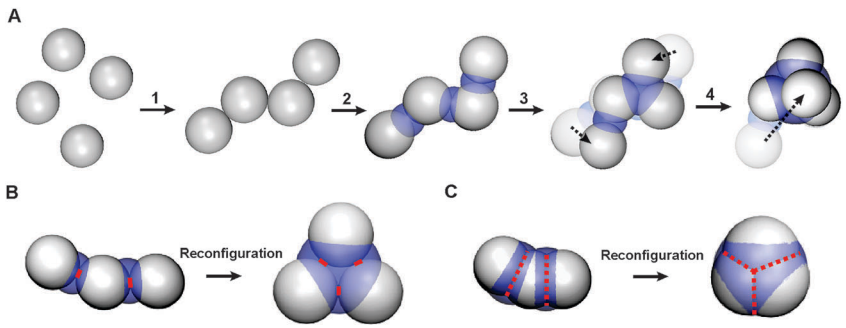

Fig. 1 (A) Illustration of the colloidal recycling method. (1) Destabilization of colloids resulting in the formation of aggregates. (2) By the addition of organic solvent (blue) to a random aggregate of four spheres, droplets of solvent are deposited at the contact area between the spheres. (3–4) The van der Waals attractions between the spheres are decreased, which enables the rotational mobility of the aggregate leading to the coalescence of the droplets for minimizing the interfacial energy of the droplet with the surrounding water. The obtained compact cluster is spanned by a single droplet creating a patchy particle. Illustrations of trimers of rigid (B) and deformable (C) spheres with the contact areas highlighted in red. The contact area between the rigid spheres is small and the shape of these spheres is largely preserved after reconfiguration. The soft spheres are largely deformed by the strong capillary forces induced by the organic droplets, which results in large contact areas and compact patchy particle shapes.

Open Access Article. Published on 04 January 2018. Downloaded on 1/15/2026 5:10:06 AM.
This article is licensed under a Creative Commons Attribution 3.0 Unported Licence.

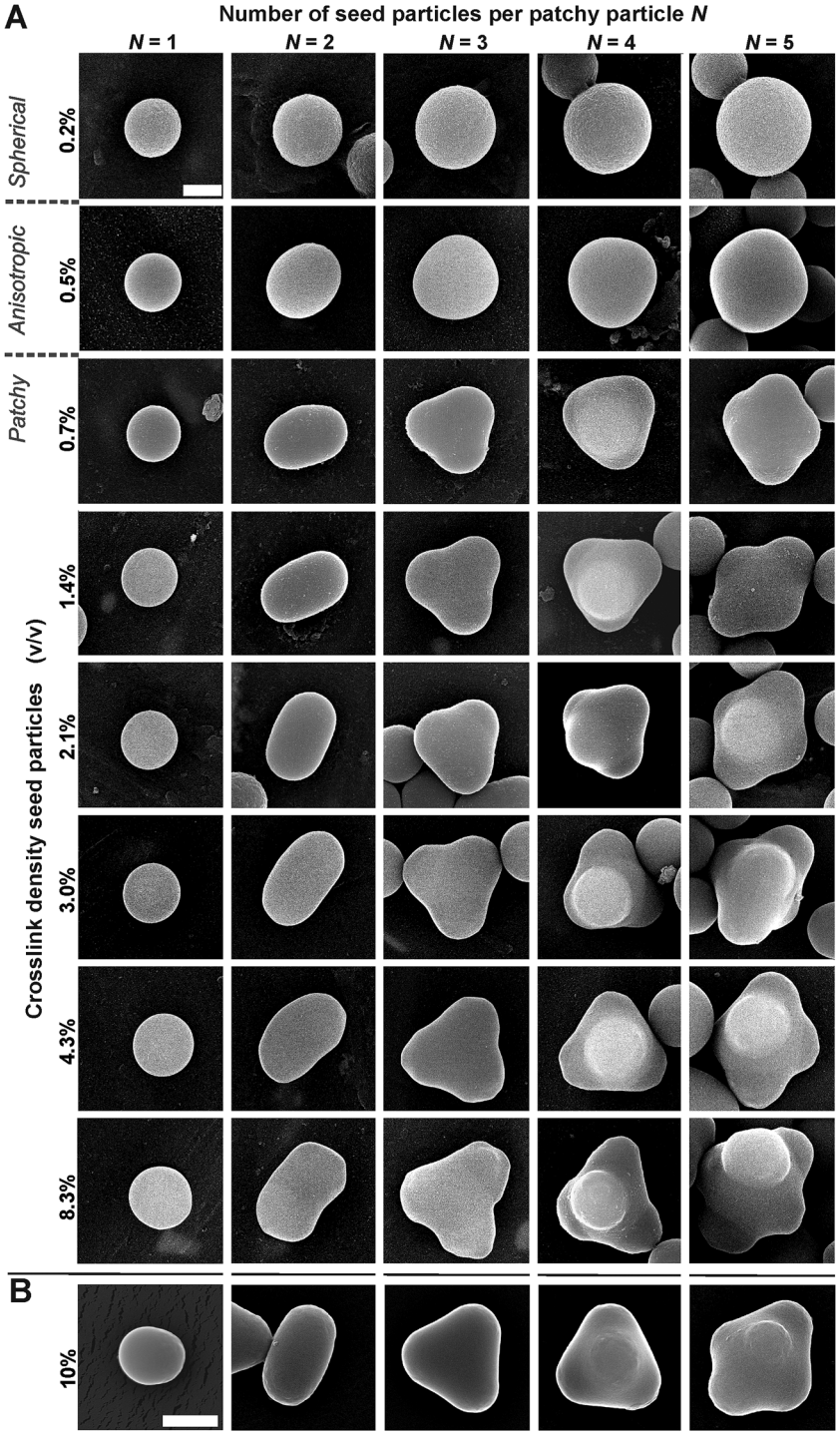

Fig. 2 SEM micrographs of spherical, anisotropic and patchy particles of N = 1–5 formed by polystyrene seed particles of different crosslink densities (cd). Scale bar is 1 μm. (A) Particles constructed by spheres of fixed crosslink density, ranging from 0.2% v/v at the top row to 8.3% v/v at the bottom row. The seeds are all synthesized following the same emulsion polymerization protocol. Per column particles consisting of a fixed number of seed particles are shown. At 0.2% v/v cd the seed particles completely merge during reconfiguration, which yields spheres with a larger diameter. Spheres with 0.5% v/v cd slightly resist deformation, resulting in anisotropic particles. At higher cd, 0.7 $\leq$ cd $\leq$ 8.3% v/v, the shape of the seeds is largely preserved and patchy particles are formed. Spheres with very densely crosslinked polymer networks, 4.3 or 8.3% v/v cd, form patchy particles with irregular features at the patches. (B) Patchy particles constructed from 10% v/v crosslinked 1.06 μm seed particles purchased from Magsphere Inc. Large field of view SEM micrographs of the reconfigured particles are shown in Fig. S3 (ESI†).

spheres merged completely into a single, larger sphere (Fig. 2 row 1) to minimize the interfacial energy between the organic solvent and the water phase. Spheres with 0.5% v/v crosslinking agent were sufficiently rigid to partly resist the strong capillary forces acting on the seeds, resulting in anisotropic shapes with a smooth surface (Fig. 2 row 2).

 This journal is © The Royal Society of Chemistry 2018

Open Access Article. Published on 04 January 2018. Downloaded on 1/15/2026 5:10:06 AM.
This article is licensed under a Creative Commons Attribution 3.0 Unported Licence.

Seeds with more densely crosslinked polymer networks, $0.7 \leq cd \leq 8.3\%$ v/v, deformed less during reconfiguration compared to the poorly crosslinked seeds. Here, well-defined particles were obtained where part of the original spheres could be identified as patches protruding from the central body formed by polymerization of the styrene droplet (Fig. 2 row 3–8 and Fig. S2, ESI†). Since the seed particles and the organic droplet consist of similar material, the patches have a low wetting angle with the body. This results in a rather continuous boundary between the two phases. We identified the position of this boundary by the difference in contrast and surface morphology between the patches and the body in SEM micrographs. When no distinction could be made the particles were identified as non-patchy. For patchy particles of a given number of constituent spheres ($N \leq 5$) the same shape was obtained: the dumbbell for $N = 2$, triangle for $N = 3$, tetrahedron for $N = 4$ and the triangular dipyramid for $N = 5$. These structures have previously been observed for clusters of spheres obtained through an evaporation-driven assembly,[32,33,37] long-range Lennard Jones 6–12 potentials,[28] short-range interactions,[27,30] capillary bridges,[25,38] and hydrophobic patchy interactions.[5]

Although rarely observed we note that some patchy particles have slight deviations from these geometries. Illustrative is the triangular dipyramid constructed from seeds with a 3.0% v/v crosslink density (Fig. 2 row 6). These small deviations in geometry may be attributed to the polydispersity of the seed particles in size and surface properties or inhomogeneities in the crosslinked polymer network.[35,39] The latter may also cause the formation of the irregular features arising at the patches at a significant crosslink density, cd = 4.3 or 8.3% v/v (Fig. 2 row 7–8). These irregularities are likely protrusions or local deformations of the seeds.

Further examination of patchy particles constructed from seeds with 0.7 and 8.3% v/v cd reveals that the body of the patchy particle, originating from the cluster-spanning droplet, engulfs a different fraction of the original seeds (see Fig. S2, ESI†). While for the soft particles only a small part of the spheres protrudes from the body, a large part of the rigid spheres is visible. This difference is likely caused by a deformation of the spheres in the contact area and at the interfaces of the droplet and solvent.[40] The degree of deformation decreases with increasing crosslink density. In addition, the crosslink density can influence the contact angle of the particles with the styrene droplet as well as the degree of swelling during droplet deposition and thus the volume of the cluster-spanning droplet.[35,41] The crosslink density therefore may impact the degree of protrusion of the seed particles from the body of the patchy particles in multiple ways.

The crosslink density also affected the size distribution of the resulting particles. SEM micrographs of the dispersions of the reconfigured particles are shown in Fig. S3 (ESI†). The size distributions of the particles constructed by seeds with cd = 0.7, 4.3 and 8.3% v/v are shown in Fig. S4 (ESI†). These distributions are set during the aggregation step.[26] For all size distributions the probability of finding a sphere in a cluster of size N decreases with increasing cluster size. The size distribution shifts to larger cluster sizes with increasing crosslink density. This indicates that the DVB concentration in the seeds changes the surface properties of the particles.

Shape deformation analysis of dumbbells

To study the relation between the crosslink density and the deformability of the spheres, we analyzed the shape of the dumbbells. SEM micrographs of multiple dumbbells formed by seeds with crosslink densities ranging from 0.2–8.3% v/v are shown in Fig. S5 (ESI†). We quantified the deformation of the colloidal dumbbells by measuring the aspect ratio between the long and the short axis, the length L and width W, respectively (see Fig. 3 inset). When two seed particles merge completely into a larger sphere, L and W are equal and therefore L/W equals 1. The higher the value of the aspect ratio the more aspherical is the dumbbell and thus the less deformed are the spheres. The plot in Fig. 3 presents the aspect ratios for dumbbells formed by seeds of crosslink densities ranging from 0.2–8.3% v/v. Slightly larger error bars are observed at 4.3% and 8.3% v/v cd due to the surface inhomogeneities of the patches. Yet, we found a maximum polydispersity in the L/W ratio of only 6% for any crosslink density. This shape consistency arises from the uniform properties of the seed particles such as the swelling capacity, size and wetting angle with the droplet. The low polydispersity of the dumbbells is in line with previous measurements of trimer particles, where the polydispersity in the center-to-center distance of the spheres in the trimers was also only 5.8%.[26]

The data in Fig. 3 show that L/W increases with the crosslink density, indicating that the deformation depends strongly on the density of the crosslinked polymer network.[36,42] By least-squares fitting the data to $y = B - A \cdot \exp(-cd/C)$, where cd is the crosslink density of the seeds and y the aspect ratio L/W, we find $B = 1.75$, $A = 0.87$ and $C = 1.00$. The saturation value at high crosslink densities, here 1.75, corresponds to a dumbbell of

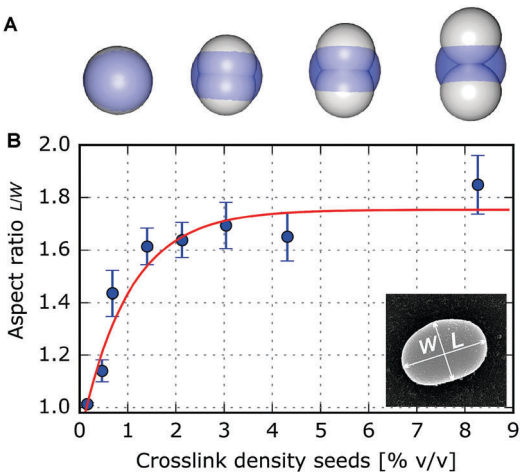

Fig. 3 Deformation of dumbbells. (A) Illustration of the effect of capillary forces on the shape of dumbbells constructed from deformable spheres. Sphere deformability decreases from left to right. (B) The aspect ratio, L/W, of dumbbells increases with the crosslink density of the seeds. This indicates that the seed particles are less deformed upon reconfiguration at increasing rigidity. The red line is the result of a least squares fit of the data, $y = 1.75 - 0.87 \cdot \exp((-cd)/1.00)$.

Open Access Article. Published on 04 January 2018. Downloaded on 1/15/2026 5:10:06 AM.
This article is licensed under a Creative Commons Attribution 3.0 Unported Licence.

non-deformed spheres. Since L_{max} is equal to two times the radius of the seeds, this saturation value is determined by the thickness of the polystyrene body, which depends on the properties of the seeds such as their wetting angle with the styrene droplet as well as the swelling ratio.

A similar analysis was performed by Pawar *et al.* to measure the degree of merging of two 100 μm elastic oil droplets.[43] The rigidity in these droplets originated from wax crystals incorporated in the oil, where the elastic modulus increased with the wax concentration. They further calculated the strain ε, which is defined as the difference between the lengths of the long axis of the dumbbell before and after coalescence, ΔL, divided by the initial length L_0. We obtained qualitatively similar results to those of the non-Brownian elastic droplets, although a quantitative comparison is not possible since this analysis method cannot be applied to our colloidal dumbbells. The reason is that ΔL is influenced by the volume increase of the spheres during swelling with organic solvent and the degree of swelling also depends on the crosslink density of the seeds.[35] Pawar *et al.* found that the degree of deformation depended on the balance between the elasticity of the droplets and the interfacial energy, where total coalescence was observed for droplets with a low elasticity, $\varepsilon = 0.37$, and the total stability for elastic droplets, $\varepsilon = 0$. We observed that two colloids of low crosslink density and thus low rigidity also completely coalesced resulting in an aspect ratio L/W equal to 1. At increasing crosslink density the particles are increasingly able to resist deformation leading to higher L/W values, up to a saturation value of 1.75.

Patch arrangements for particles of $N > 5$

While for particles shaped from up to five spheres a fixed geometry is observed for each cluster size, the arrangement of larger clusters depends on the underlying organizing principle such as packing constraints,[32] particle wettability,[33] interaction potential[28,29] and entropic effects.[30] For $N = 6$ this may lead to a polytetrahedral or octahedral structure. Surprisingly, in our initial study[26] we have observed both the octahedral and the polytetrahedral arrangement of the patches for different batches of seed particles.[26] This points towards the fact that the physical and/or chemical properties of the seeds play an important role in determining the outcome of the reconfiguration process. Because the two batches of particles strongly differed in the particle softness, we have speculated that the rigidity may be origin of the observed difference.

To single out the effect of particle rigidity we here investigated the patch arrangements for polystyrene seeds with crosslink densities 0.7, 2.1, 4.3 and 8.3% v/v synthesized following the same protocol. The patchy particles resulting from the reconfiguration process exhibit a striking transition from the polytetrahedron at low crosslink density to the octahedron at high crosslink density (Fig. 4A). Clusters of six seeds with a low crosslink density, cd = 0.7% v/v, reconfigured only into the polytetrahedron. At 2.1% v/v

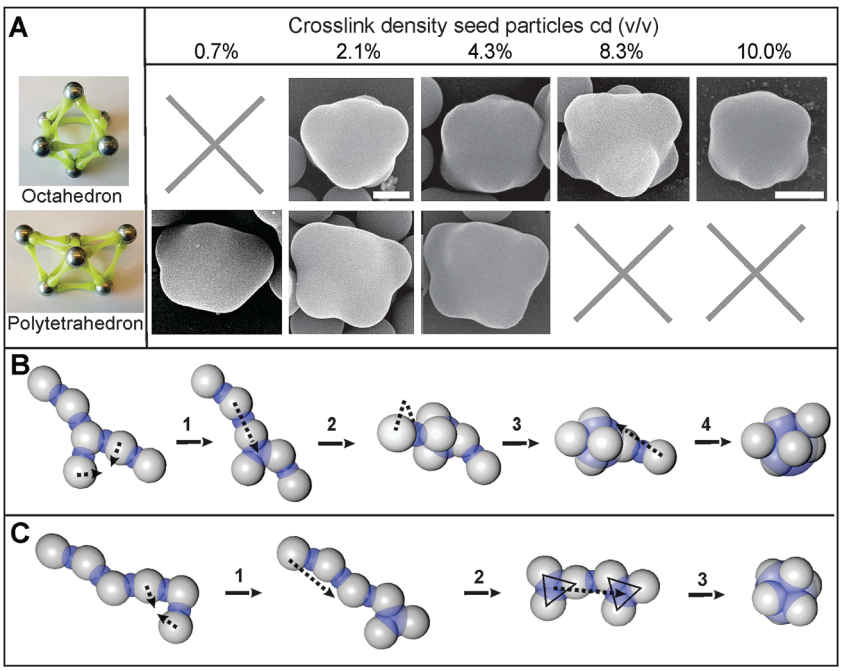

Fig. 4 Patch arrangements and reconfiguration pathway of patchy particles of $N = 6$. (A) Schematic illustration and SEM micrographs of the octahedron (top row) and the polytetrahedron (bottom row) constructed from seed particles with cd = 0.7%, 2.1%, 4.3%, 8.3% and 10% v/v cd. The seed particles with 10% v/v crosslink density are commercially purchased from Magsphere Inc. and synthesized by a different procedure. The octahedron is not formed by spheres with a low crosslink density and the polytetrahedron is not observed for rigid spheres. Scalebar is 1 μm. (B) Illustration of the reconfiguration pathway of a cluster of six spheres into the polytetrahedron. Upon coalescence of the small droplets into a larger droplet subsequently a triangle, step 1, and a tetramer, step 2, are formed. From the tetrahedron the reconfiguration continues leading to the triangular dipyramid, step 3, and eventually the polytetrahedron with a single droplet spanning the cluster, step 4. (C) Reconfiguration pathway leading to the octahedron geometry. To form this geometry two trimers have to be formed, without the formation of a tetramer, which assemble on top of each other to yield the octahedron. The formation of the octahedron is therefore less likely to occur compared to the polytetrahedron.

 This journal is © The Royal Society of Chemistry 2018

Open Access Article. Published on 04 January 2018. Downloaded on 1/15/2026 5:10:06 AM.
This article is licensed under a Creative Commons Attribution 3.0 Unported Licence.

crosslink density the polytetrahedron was formed predominantly, while at 4.3% v/v mainly the octahedron was observed. At 8.3% v/v crosslink density we only found the octahedron. This is in line with what we had observed previously for patchy particles made from highly crosslinked (10% v/v) 1.06 μm polystyrene particles obtained from Magsphere Inc., which also only show the octahedral arrangement. Clearly, an increase in the crosslink density induces the transition from the polytetrahedral to the octahedral arrangement.

For $N > 6$ the number of possible arrangements increases dramatically with each additional sphere. Already for patchy particles consisting of $N = 7$ spheres, it becomes difficult to distinguish the different arrangements from 2D SEM images. In experiments and free energy calculations of clusters of seven spheres with short range attractions six geometries were observed, see Fig. 5A for point group notations and illustrative models. Fig. 5A also shows the sides of a polytetrahedron where the seventh sphere is positioned to form the $N = 7$ structures. Qualitatively, we observe that the rigid spheres with cd = 10% v/v arrange in all these geometries, with the pentagonal dipyramid (D_{5h} and C_{2v}) structures being dominant (Fig. 5B). Spheres of 0.7% v/v cd do only rarely achieve the pentagonal dipyramid structures and predominantly form the C_2 and C_{3v} point group clusters (Fig. 5C). For even larger clusters ($N > 15$), we find that the rearranged structures take up slightly elongated spherical shapes (see Fig. 6) which occasionally feature protruding spheres or bulges. This suggests that the reconfiguration got arrested in a non-equilibrium state. The final shape of large clusters is therefore largely dependent on the reconfiguration pathway.

Previous experiments and numerical analyses on particle-covered droplets found that the preferred arrangement of the spheres depends on the particle wettability and the droplet volume.[31] Similarly, for the formation of clusters upon slow droplet evaporation it was found that the final configurations arise almost entirely from geometric constrains during the drying process and depend on particle wettability.[32,44,45] The latter process inherently leads to compact clusters, possibly with several spheres inside the cluster. Our reconfiguration approach is different from earlier work in that it is essentially a bottom-up assembly of particles connected by capillary bridges that merge into a larger droplet instead of a top down approach, which starts with the adsorption of multiple spheres on a single, large droplet. Equilibrium wetting arguments alone may not be sufficient to explain our observations since capillary interactions and kinetic effects are expected to be important as well. We therefore consider the reconfiguration process itself.

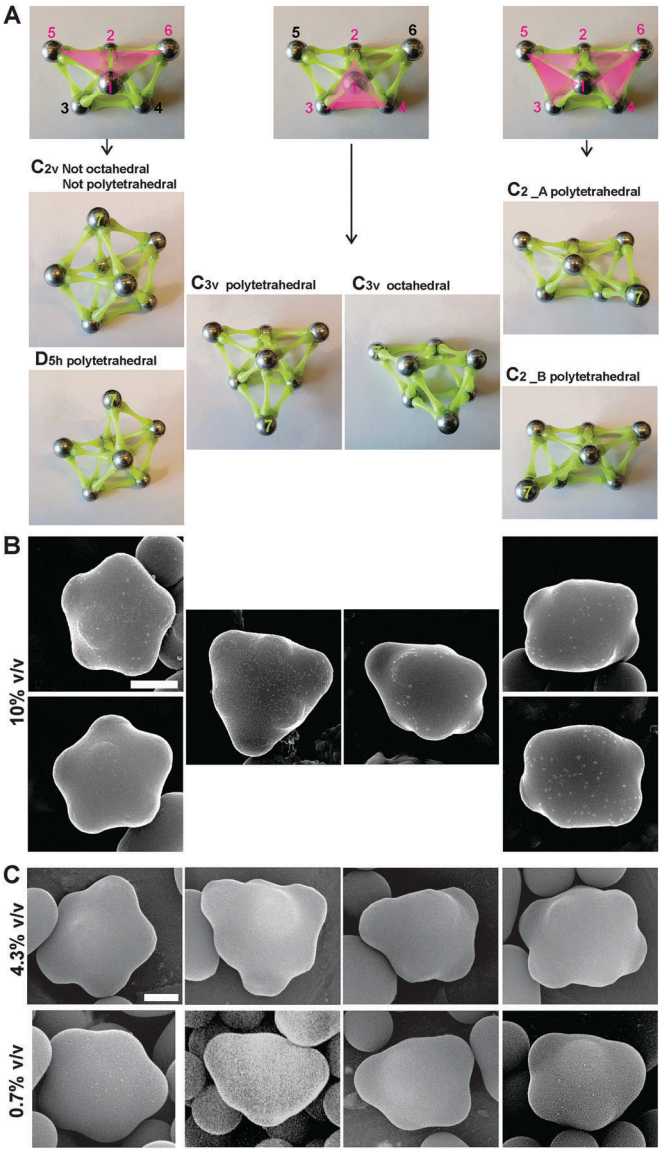

Fig. 5 (A) Models of typical minimal free energy geometries for clusters of $N = 7$. The Schönflies notation is written above the image. Above the $N = 7$ models a polytetrahedron is shown in magenta at the position where the seventh sphere can be positioned to form the $N = 7$ structures. The pentagonal dipyramids C_{2v} and D_{5h} can be differentiated by the subtle bond distance between the two spheres on the pentagon, $1.09d$ *vs.* $1.05d$, respectively, where d is the diameter of the sphere. C_{3v} has a polytetrahedral and an octahedral version. The polytetrahedral C_2 geometry has two chiral enantiomers. (B and C) SEM images of patchy particles constructed from seven spheres of different crosslink densities. Scalebars are 1 μm. (B) For patchy particles of spheres with 10% v/v crosslink density, purchased from Magsphere Inc., all six $N = 7$ geometries can be identified and these rigid spheres predominantly reconfigure into the pentagonal dipyramid geometries (C_{2v} and D_{5h}). (C) Patchy particles of 4.3% reconfigure into all geometries although we were unable to distinguish between the C_{2v} and D_{5h} geometry and only one C_2 structure is shown. At a low crosslink density, 0.7% v/v, the pentagonal dipyramids C_{2v} and D_{5h} are rarely observed.

Reconfiguration pathway

After deposition of the droplets at the contact areas of the spheres, the consecutive merging of the droplets due to the capillary interactions determines the step-wise folding into the compact structure. Crucial for coalescence and thus reconfiguration to occur is a sufficient volume of the droplets. We have studied the effect of the amount of organic liquid on the reconfiguration process previously by adding different volumes of organic liquid to the colloidal aggregates.[26] The volume was tuned by the swelling ratio S, which is defined as the mass of the organic solvent added/mass of the polymer particles. At $S < 4$, reconfiguration did not occur likely because the droplets at the contact areas between the

Open Access Article. Published on 04 January 2018. Downloaded on 1/15/2026 5:10:06 AM.
This article is licensed under a Creative Commons Attribution 3.0 Unported Licence.

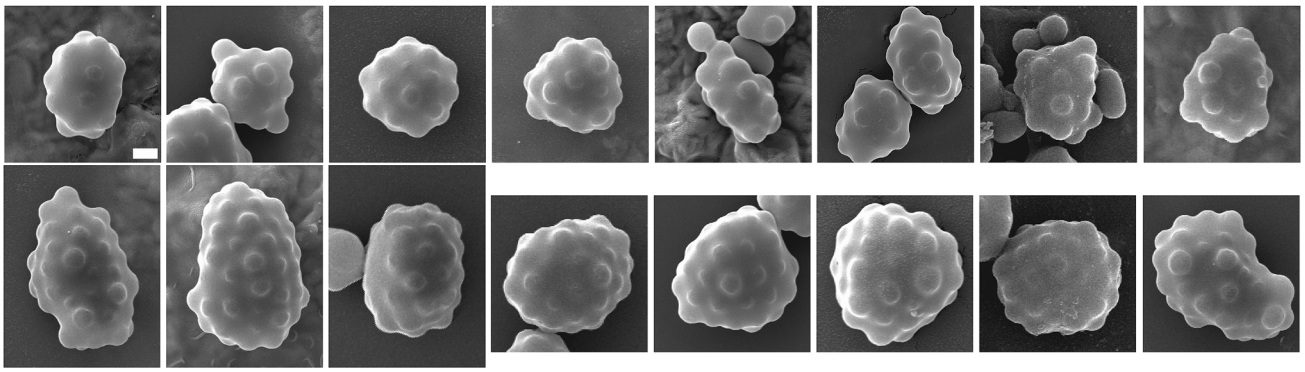

Fig. 6 SEM micrographs of patchy particles of $N > 15$ constructed from 1.06 μm seed particles with 10% v/v crosslink density. Scalebar is 1 μm. The patchy particles are of non-spherical, often elongated shapes. Protruding spheres and bulges are visible, suggesting that the reconfiguration got arrested in a non-equilibrium state. The final shape is therefore dependent on the reconfiguration pathway.

spheres were too small to merge into a larger droplet. At $S \geq 4$ reconfiguration occurred. Here, we employed $S = 8$ to ensure a high success rate for reconfiguration.

For simplicity, we examine the reconfiguration of a random aggregate of $N = 6$ spheres more closely, but similar arguments should hold for aggregates containing more spheres as well. Initially, the coalescence of two droplets yields triangular arrangements, see Fig. 4B. This may happen at any location in the aggregate, and we randomly chose one for illustration purposes in Fig. 4B. The merging of the capillary bridge of a fourth and fifth sphere and subsequent minimization of the droplet interface leads to a tetrahedral and triangular dipyramid arrangement, respectively, as was seen for the $N = 4$ and $N = 5$ clusters (Fig. 2). The rearrangement of the final sphere results in a polytetrahedral geometry through local minimization of the interface, at least in the first instance. While there exist many possible routes towards the polytetrahedron due to different possible starting locations, the assembly of an octahedral arrangement requires either the formation of two triangles and their subsequent stacking (see Fig. 4C), or a rearrangement of the polytetrahedral structure.

The capillary interactions that drive the reconfiguration are not only very strong but they are also long-ranged.[46,47] We are not aware of any predictions of the ground states of clusters of spheres interacting through capillary interactions, but presumably they are similar to the lowest energy state for spheres with long-ranged attractions, such as a Lennard-Jones 6–12 potential.[28] In this case, the ground states are the octahedron for $N = 6$ and the pentagonal dipyramid (D_{5h}) for $N = 7$. If the volume of the cluster-spanning droplet exceeds a critical value, capillary interactions can drive this rearrangement from the polytetrahedral state to the octahedron or pentagonal dipyramid.

Why do we observe the rearrangement only for rigid spheres? There are a number of possible explanations. The more crosslinked the seed particles the better they resist deformation and disintegration by the organic liquid. They also protrude more from the droplet. This implies that they occupy less volume inside the droplet, which makes rearrangements already at a lower droplet volume possible. Furthermore, since rigid spheres likely experience less friction at their smaller contact areas than the soft spheres (Fig. 1B and C), a rearrangement from the polytetrahedral to the octahedral state or pentagonal dipyramid should also be significantly easier with increasing crosslink density. Conversely, the strong deformation of the soft spheres in the presence of the confining droplet may impose additional geometric constraints that prevent rearrangement. The additional contribution from the elastic energy may render the polytetrahedral arrangement the state with the lowest energy for the softer spheres. Theoretical considerations or simulations may give conclusive insights.

Interestingly, we observed that particles with a higher crosslink density showed irregular features on the surface and these impede the reconfiguration process. We found that the probability to find a not-fully reconfigured cluster increased with the crosslink density. For smooth spheres with cd = 0.7% v/v this probability is only 1% and it increased to 8% and 12% for spheres with small (cd = 4.3% v/v) and large (cd = 8.3% v/v) surface irregularities, respectively. Still, when six rigid spheres do reconfigure, we always observe the octahedron.

The fact that the reconfiguration pathway naturally leads to polytetrahedral arrangements can be exploited for creating particles with unusual patch arrangements. By tuning the deformability of the seed particles, we therefore were able to switch from patchy particles with six patches in an octahedral to a polytetrahedral arrangement.

Conclusions

A large variety of colloids can be formed by reconfiguration of random aggregates of deformable seed particles through capillary interactions. The final shape of the particles depends on the crosslink density of the seeds, since this influences the balance between interfacial energy and the shape-conserving forces due to particle rigidity. A quantitative analysis of the dumbbell shape aspect ratio reveals that the deformation of the original spheres decreases with increasing crosslink density. Seed particles with a poorly crosslinked polymer network deform strongly during

 This journal is © The Royal Society of Chemistry 2018

Open Access Article. Published on 04 January 2018. Downloaded on 1/15/2026 5:10:06 AM.
This article is licensed under a Creative Commons Attribution 3.0 Unported Licence.

reconfiguration due to strong capillary forces that drive to minimize the interfacial energy between the water and the organic solvent. The resulting particles are spherical or slightly anisotropic. At higher crosslink densities well-defined patchy particles are obtained for clusters of $N = 1$–5.

Interestingly, the deformability of the seed particles also influences the reconfiguration pathway for larger clusters, leading to distinct geometries. Clusters of six strongly deformable colloids arrange in the polytetrahedron, while rigid particles rearrange into the octahedron. For seven spheres, the rigid particles were found in pentagonal dipyramids, whereas the soft spheres only rarely achieve this structure since the number of pathways to form this geometry is lower compared to other configurations for $N = 7$. We put forward the notion that initial compaction leads to polytetrahedral configurations and that it can be followed by a rearrangement into the state of lowest energy driven by capillary interactions. Geometric constraints, friction and the assembly path all are likely to affect the structure of the resulting patchy particles. The rigidity of the seeds is therefore a tool to guide the reconfiguration of the cluster to the desired structure.

Experimental

Materials

Styrene (≥99%, contains 4-*tert*-butylcatechol as inhibitor), divinylbenzene (DVB, technical grade 55%), azobisisobutyronitril (AIBN, ≥98%), hydroquinone (HQ, ≥99.5%), sodium dodecyl sulfate (SDS, ≥98.5%) and perylene (sublimed grade, ≥99.5%) were purchased from Sigma-Aldrich. Styrene was passed through an inhibitor remover column (Sigma-Aldrich) before use. Potassium chloride (>99% p.a.) was obtained from Fluka, Germany.

The water used was deionized using a Millipore Filtration System (MilliQ Gradient A10), resulting in a resistivity of 18.2 MΩ cm.

Seed particle synthesis

Linear carboxylic acid functionalized polystyrene spheres of 1.05 ± 0.02 μm in diameter were synthesized by a surfactant free emulsion polymerization procedure.[48] The colloids were stored in water after filtration over glass wool and washing. To 13.5 mL of a 2.29 wt% dispersion of these linear seeds, 0.05 g SDS, 0.034 g HQ and 1.7 mL crosslink solution was added to swell and crosslink the particles. The crosslink solution consisted of styrene with 2 wt% AIBN and 0.2, 0.6, 1, 2, 3, 4, 6 or 10% v/v DVB, yielding seed particles with different crosslink densities. The mixtures were rotated for 24 h on a tumbler at 20 rpm in the dark. Finally, the swollen colloids were polymerized in a 72 °C preheated oil bath for 24 h while being rotated at 100 rpm at a 45° angle. The synthesized particles had a smooth surface morphology and a polydispersity below 4%. They were washed and stored in water. The characteristics of all synthesized particles are listed in Table 1 and SEM micrographs are displayed in Fig. S1 (ESI†).

Table 1 Characteristics of polystyrene seed particles synthesized including the diameter the concentration DVB, [DVB] in the crosslink solution and the [DVB] in the final seed which corresponds to the crosslink density of the final seed

[DVB] crosslink solution [% v/v]	[DVB] final seed [% v/v]	Diameter [μm]
0.0	0.00	1.05 ± 0.02
0.2	0.16	1.57 ± 0.04
0.6	0.46	1.53 ± 0.06
1.0	0.68	1.42 ± 0.03
2.0	1.40	1.44 ± 0.04
3.0	2.13	1.45 ± 0.05
4.0	3.04	1.51 ± 0.02
6.0	4.31	1.46 ± 0.04
10.0	8.27	1.61 ± 0.05

In addition, the RITC dyed polystyrene spheres of 1.06 ± 0.06 μm with a crosslink density of 10% v/v were purchased from Magsphere Inc.

Patchy particle preparation method

Patchy particles were prepared using the 'colloidal-recycling' method.[26] Here, random aggregates are formed first by diffusion limited aggregation. Aggregation was induced by the addition of 100 μL of a 2 M potassium chloride solution to a 100 μL electrostatically stabilized colloidal suspension (4.4 wt%). After an aggregation time, t_a, of 2 min the dispersion was quenched with 15 mL water. To obtain clusters of $N > 15$, the spheres purchased from Magsphere Inc. were aggregated for 8 min before quenching.

The random aggregates were reconfigured into compact clusters by the addition of an organic solvent: to 5 mL of a quenched dispersion containing random aggregates, 10 μL of aqueous SDS solution (10 wt%) and 12.7 μL of a reconfiguration solution, consisting of styrene with 1.5% v/v DVB and 2 wt% AIBN, was added. The swelling ratio S, defined as the mass of the organic solvent/the mass of the polymer colloids in these experiments was 8, which was sufficient to achieve reconfiguration.[26] The dispersion was magnetically stirred for 24 h to complete the reconfiguration of the aggregates. The obtained patchy particles were polymerized for 24 h in a preheated oil bath at 80 °C. The particles were washed and stored in water.

Imaging and analysis

The synthesized polystyrene seed particles and polymerized patchy particles were imaged using a FEI nanoSEM scanning electron microscope (SEM) at 80 kV. The size of the linear and crosslinked seed particles was determined by measuring the circumference of >100 particles in SEM micrographs with ImageJ. ImageJ was also used for the analysis of patchy particles of $N = 2$ formed by seed particles of different crosslink densities. Here the long axis ("length") and the short axis ("width") of the dumbbell were measured of at least 30 particles per sample. For each particle the l/w ratio was determined and averaged.

Conflicts of interest

There are no conflicts to declare.

Open Access Article. Published on 04 January 2018. Downloaded on 1/15/2026 5:10:06 AM.
This article is licensed under a Creative Commons Attribution 3.0 Unported Licence.

Acknowledgements

We thank C. van der Wel for providing the linear carboxylic acid functionalized polystyrene spheres. We also gratefully acknowledge funding through the VENI Grant 680-47-431 by the Netherlands Organization for Scientific Research (NWO).

Notes and references

1 G.-R. Yi, D. J. Pine and S. Sacanna, *J. Phys.: Condens. Matter*, 2013, **25**, 193101.
2 F. Li, D. P. Josephson and A. Stein, *Angew. Chem., Int. Ed.*, 2011, **50**, 360–388.
3 S. Sacanna, D. J. Pine and G.-R. Yi, *Soft Matter*, 2013, **9**, 8096–8106.
4 D. J. Kraft, R. Ni, F. Smallenburg, M. Hermes, K. Yoon, D. A. Weitz and A. Van Blaaderen, *Proc. Natl. Acad. Sci. U. S. A.*, 2012, **109**, 10787–10792.
5 Q. Chen, J. K. Whitmer, S. Jiang, S. C. Bae, E. Luijten and S. Granick, *Science*, 2011, **331**, 199–202.
6 J. R. Wolters, G. Avvisati, F. Hagemans, T. Vissers, D. J. Kraft, M. Dijkstra and W. K. Kegel, *Soft Matter*, 2015, **11**, 1067–1077.
7 E. Bianchi, C. N. Likos and G. Kahl, *ACS Nano*, 2013, **7**, 4657–4667.
8 F. Smallenburg and F. Sciortino, *Nat. Phys.*, 2013, **9**, 554–558.
9 Z. Zhang, A. S. Keys, T. Chen and S. C. Glotzer, *Langmuir*, 2005, **21**, 11547–11551.
10 E. G. Noya, C. Vega, J. P. Doye and A. A. Louis, *J. Chem. Phys.*, 2010, **132**, 234511.
11 X. Mao, Q. Chen and S. Granick, *Nat. Mater.*, 2013, **12**, 217–222.
12 F. Sciortino, E. Bianchi, J. F. Douglas and P. Tartaglia, *J. Chem. Phys.*, 2007, **126**, 194903.
13 L. Lu, X. Li, P. G. Vekilov and G. E. Karniadakis, *Biophys. J.*, 2016, **110**, 2085–2093.
14 J. J. Mcmanus, P. Charbonneau, E. Zaccarelli and N. Asherie, *Curr. Opin. Colloid Interface Sci.*, 2016, **22**, 73–79.
15 F. Romano, E. Sanz and F. Sciortino, *J. Phys. Chem. B*, 2009, **113**, 15133–15136.
16 P. F. Damasceno, M. Engel and S. C. Glotzer, *Science*, 2012, **337**, 453–457.
17 S. H. Kim, G. R. Yi, K. H. Kim and S. M. Yang, *Langmuir*, 2008, **24**, 2365–2371.
18 D. J. Kraft, W. S. Vlug, C. M. Van Kats, A. Van Blaaderen, A. Imhof and W. K. Kegel, *J. Am. Chem. Soc.*, 2009, **131**, 1182–1186.
19 Y.-S. Cho, G.-R. Yi, J.-M. Lim, S.-H. Kim, V. N. Manoharan, D. J. Pine and S.-M. Yang, *J. Am. Chem. Soc.*, 2005, **127**, 15968–15975.
20 A. Desert, C. Hubert, Z. Fu, L. Moulet, J. Majimel, P. Barboteau, A. Thill, M. Lansalot, E. Bourgeat-lami, E. Duguet and S. Ravaine, *Angew. Chem.*, 2013, **52**, 11068–11072.
21 Y. Wang, Y. Wang, D. R. Breed, V. N. Manoharan, L. Feng, A. D. Hollingsworth, M. Weck and D. J. Pine, *Nature*, 2012, **491**, 51–55.
22 X. Zheng, Y. Wang, Y. Wang, D. J. Pine and M. Weck, *Chem. Mater.*, 2016, **28**, 3984–3989.
23 Y. Wang, A. D. Hollingsworth, S. K. Yang, S. Patel, D. J. Pine and M. Weck, *J. Am. Chem. Soc.*, 2013, **135**, 14064–14067.
24 Q. Chen, S. C. Bae and S. Granick, *Nature*, 2011, **469**, 381–384.
25 B. Bharti, D. Rutkowski, K. Han, A. U. Kumar, C. K. Hall and O. D. Velev, *J. Am. Chem. Soc.*, 2016, **138**, 14948–14953.
26 V. Meester, R. W. Verweij, C. van der Wel and D. J. Kraft, *ACS Nano*, 2016, **10**, 4322–4329.
27 N. Arkus, V. N. Manoharan and M. P. Brenner, *Phys. Rev. Lett.*, 2009, **103**, 118303.
28 M. R. Hoare and P. Pal, *Adv. Phys.*, 1971, **20**, 161–196.
29 S. Mossa, F. Sciortino, P. Tartaglia and E. Zaccarelli, *Langmuir*, 2004, **20**, 10756–10763.
30 G. Meng, N. Arkus, M. P. Brenner and V. N. Manoharan, *Science*, 2010, **327**, 560–563.
31 E. Koos and N. Willenbacher, *Soft Matter*, 2012, **8**, 3988–3994.
32 V. N. Manoharan, M. T. Elsesser and D. J. Pine, *Science*, 2003, **301**, 483–487.
33 E. Lauga and M. P. Brenner, *Phys. Rev. Lett.*, 2004, **93**, 238301.
34 Y. Min, M. Akbulut, K. Kristiansen, Y. Golan and J. Israelachvili, *Nat. Mater.*, 2008, **7**, 527–538.
35 H. R. Sheu, M. S. El-Aasser and J. W. Vanderhoff, *J. Polym. Sci., Part A: Polym. Chem.*, 1990, **28**, 629–651.
36 Y. G. Durant and D. C. Sundberg, *Macromolecules*, 1996, **29**, 8466–8472.
37 C. S. Wagner, Y. Lu and A. Wittemann, *Langmuir*, 2008, **24**, 12126–12128.
38 D. J. Kraft, W. S. Vlug, C. M. Van Kats, A. Van Blaaderen, A. Imhof and W. K. Kegel, *J. Am. Chem. Soc.*, 2008, **131**, 1182–1186.
39 D. J. Kraft, J. Hilhorst, M. A. P. Heinen, M. J. Hoogenraad, B. Luigjes and W. K. Kegel, *J. Phys. Chem. B*, 2011, **115**, 7175–7181.
40 H. Mehrabian, J. Harting and J. H. Snoeijer, *Soft Matter*, 2016, **12**, 1062–1073.
41 B. G. P. Van Ravensteijn and W. K. Kegel, *J. Colloid Interface Sci.*, 2017, **490**, 462–477.
42 J. W. Kim, R. J. Larsen and D. A. Weitz, *Adv. Mater.*, 2007, **19**, 2005–2009.
43 A. B. Pawar, M. Caggioni, R. W. Hartel and P. T. Spicer, *Faraday Discuss.*, 2012, **158**, 341–350.
44 G.-R. Yi, V. N. Manoharan, E. Michel, M. T. Elsesser, S.-M. Yang and D. J. Pine, *Adv. Mater.*, 2004, **16**, 1204–1208.
45 C. S. Wagner, B. Fischer, M. May and A. Wittemann, *Colloid Polym. Sci.*, 2010, **288**, 487–498.
46 P. A. Kralchevskyt and K. Nagayama, *Langmuir*, 1994, **10**, 23–36.
47 D. Stamou, C. Duschl and D. Johannsmann, *Phys. Rev. E: Stat. Phys., Plasmas, Fluids, Relat. Interdiscip. Top.*, 2000, **62**, 5263.
48 J. Appel, S. Akerboom, R. G. Fokkink and J. Sprakel, *Macromol. Rapid Commun.*, 2013, **34**, 1284–1288.

 This journal is © The Royal Society of Chemistry 2018